PERGAMON

International Journal of Hydrogen Energy 27 (2002) 863–870

International Journal of HYDROGEN ENERGY

www.elsevier.com/locate/ijhydene

Photoelectrolysis of water to hydrogen in p-SiC/Pt and p-SiC/n-TiO_2 cells

Jun Akikusa, Shahed U.M. Khan *

Department of Chemistry and Biochemistry, Dusquesne University, Pittsburgh, PA 15282, USA

Abstract

The rates of photoelectrolysis of water to hydrogen and oxygen in p-SiC/Pt cells were found to depend on the surface treatment of p-SiC by aqua-regia-HF solution and also on electrocatalytic Pt metal islet deposition. The limiting currents were not dependent on the surface treatments by aqua-regia-HF solution or Pt metal islet deposition. The optimum etching time and Pt electrodeposition time were found to be 3 min and 5 s, respectively. The electrode potential under illumination of intensity was 50 mW cm^{-2} and at open circuit condition was found to be 1.25 V Saturated calomel electrode (SCE) and was not dependent on the surface treatments. The photocurrent onset potential was found to be dependent on surface treatments. The surface treatments by etching and Pt metal islet electrodeposition shifted the onset potential, ΔE maximum by 0.27 V. The maximum photocurrent density of 0.135 mA cm^{-2} at 00 V SCE^{-1} was obtained on aqua-regia-HF etched and Pt metal islet deposited p-SiC surface. The photoconversion efficiency was found to be 0.17% at an applied potential of 0.45 V and the corresponding total conversion efficiency was 0.27%. The bandgap energy was found to be 2.92 eV for the p-SiC sample. The flat band potential of 1.42 V SCE^{-1} and the donor density of 3.8×10^{18} cm^{-3} was found from the Mott–Schottky plots at AC frequency range between 600 and 1000 Hz. The p-SiC/n-TiO_2 cells were found to photosplit water without the use of any external applied potential with maximum photocurrent density of 0.05 mA cm^{-2} and the corresponding efficiency of 0.06%. The low cell photocurrent density and the photoconversion efficiency for the p-SiC/n-TiO_2 self-driven system for the water-splitting reaction were due to high bandgap energies of both semiconductors and high recombination of photo-generated carriers mainly in the covalent bonded p-SiC. © 2002 Published by Elsevier Science Ltd on behalf of the International Association for Hydrogen Energy.

Keywords: Photoelectrolysis; Water splitting; Silicon carbide; Photoconversion efficiency; Bandgap; Electrodeposition; Metal Islets

1. Introduction

The p-SiC is one of the rarely examined p-type semiconductors [1–6] having relatively a high bandgap energy of 3.0 eV. The large bandgap and the suitable conduction band and valence band positions [7] make p-SiC important to explore its photoresponse towards water-splitting reaction. The large bandgap semiconductors are generally more stable compared to those with smaller bandgaps though they can absorb only small fraction ($\sim$ 5%) of photons of sunlight prior to proper sensitization. Furthermore, large bandgap p-type semiconductor materials are rare. The large bandgap semiconductors can provide most of the required energy for the water-splitting reaction. The n-SiC suffers photocorrosion. However, the photocorrosion problem of p-SiC may be overcome because hydrogen is formed on this photocathode and oxygen at the metal, for example Pt counter electrode in p-SiC/Pt cell or at stable n-TiO_2 electrode in p-SiC/n-TiO_2 cell. Note that we have not used n-SiC photoanode in combination with the p-SiC photocathode because of instability of the former due to its photocorrosion. Instead, we used stable n-TiO_2 as the photoanode in combination with p-SiC photocathode.

In this study we focused in determining the photoresponse of a stable and only available high bandgap p-type semiconductor, p-SiC towards water-splitting reaction in a p-SiC/Pt

* Corresponding author. Tel.: +1-412-396-1647; fax: +1-412-396-6682.

E-mail address: khan@duq.edu (S.U.M. Khan).

0360-3199/02/$ 22.00 © 2002 Published by Elsevier Science Ltd on behalf of the International Association for Hydrogen Energy.
PII: S0360-3199(01)00191-4

cell and then to find whether the combination of the stable high bandgap semiconductors, p-SiC and n-TiO_2 in a p-SiC/n-TiO_2 cell can generate enough photopotential to split water without the need of any external bias potential. Several studies [8–13] were carried out in finding the effect of surface modification by etching and also electrodeposition of electrocatalytic metal islets on p-Si and p-InP single crystals. However, such studies were not carried out on p-SiC single crystals. We focused also in this study in determining the effect of surface modification of single crystal p-SiC by etching and electrodeposition of Pt metal islets on the rate of photoelectrolysis of water to hydrogen and oxygen. Physical constants such as bandgap energy, flatband potential, donor density, and quantum efficiency were also determined for the p-SiC electrode.

2. Experimental

Pieces of p-SiC single crystal donated by Sandia National Laboratory, New Mexico, were used. The surface was cleaned by the alumina polish (Alpha micropolish 0.1 μm). The ohmic contact was made at the back side of p-SiC by the silver epoxy resin connected with copper wire and then covered by the silicon rubber adhesive.

2.1. Etching and electrodeposition of Pt islets

The surface etching of p-SiC was performed by the aqua-regia-HF-solution (HNO_3:HCl:HF = 1:3:4) for a certain time (1–6 min) to have an oxide-free surface. The platinum metal islets were deposited electrochemically on etched p-SiC surface under illumination of light. The electrolyte used for Pt deposition was 4% hydrogen hexachloroplatinate (IV), H_2PtCl_6, solution (Aldrich). A 250 μA cm^{-2} of galvanostatic current was applied for 1–8 s under light intensity of 100 mW cm^{-2} to have optimum deposition of Pt metal islets.

2.2. Photoelectrochemical measurements

The photoelectrochemical measurements were performed in a glass cell with a flat Pyrex glass window to facilitate the transmittance of light used for the photoelectrochemical measurements. The working single crystal p-SiC electrode had a surface area of 0.25 cm^2 (1.0 mm thick). A Pt wire and a saturated calomel electrode (SCE) were used as the counter and the reference electrodes, respectively. A constant intensity of 50.0 mW cm^{-2} of light from the Xenon lamp (Kratos model LH 150/1) was maintained, taking into account of the loss through the Pyrex glass window. The intensity of light was measured with a digital radiometer (model IL 1350). A monochromator (Kratos model GM 100) was used to generate the light of a particular wavelength. The electrolyte solution used for the water-splitting reaction was 0.5 M H_2SO_4. A scanning potentiostat (EG & G Princeton Applied Research, model 362) was used for the measurement of photocurrent–potential dependence. The photocurrents (which are the measure of the rate of photoelectrochemical splitting of water) as a function of electrode potential were recorded on an X–Y recorder (Houston model RE 0092). A Keithley multimeter was also used to monitor the photocurrent.

2.3. AC impedance measurements

The AC impedance of p-SiC electrode was measured using an EG & G Two-Phase Lock-In Analyzer (Model 5208) equipped with EG & G Potentiostat/Galvanostat (Model 273). These instruments were computer-controlled by EG& G software (Model 378) that automatically adjusted the phase angle during each measurement. An AC amplitude of 10 mV was used for all measurements. A Pt mesh electrode was used as the counter electrode, and the p-SiC single crystal were used as the working electrode. These measurements were carried out in the dark in 0.5 M H_2SO_4 solution.

The capacitance, C, was calculated using the following expression of impedance, Z, for a series capacitor–resistor model,

$$Z = Z' + iZ'', \tag{1}$$

where Z' is the real part of the impedance and Z'' is the imaginary part of the impedance. The capacitance, C can thus be obtained using

$$Z'' = -i/\omega C \tag{2}$$

with $\omega = 2\pi f$, $i = (-1)^{1/2}$, f is the AC frequency in Hertz. The values of Z'' at different AC frequencies were obtained from Nyquist plot (Z'' versus Z') generated from the measured data of impedance, $|Z|$, by using the EG & G software Model 378.

2.4. Synthesis of n-TiO_2 thin films

The n-TiO_2 thin films were synthesized by thermal oxidation of Ti metal sheet (Aldrich, 0.127 mm thick) in a natural glass flame in presence of oxygen gas (not in presence of air) at optimum temperature of 850 °C for the optimum time of 13 min as detailed in Ref. [15].

3. Results and discussion

3.1. The p-SiC/Pt photoelectrochemical cell

3.1.1. Photocurrent–potential dependence

The dependence of photocurrent density (j_p) and the potential (E) at p-SiC in 0.5 M H_2SO_4 is shown in Fig. 1. To remove the surface oxide, p-SiC was treated by the aqua-regia-HF solution (HNO_3:HCl:HF = 1:3:4) indicated as "Aqua-HF", then Pt metal islets were electrodeposited on the etched surface of p-SiC under illumination of

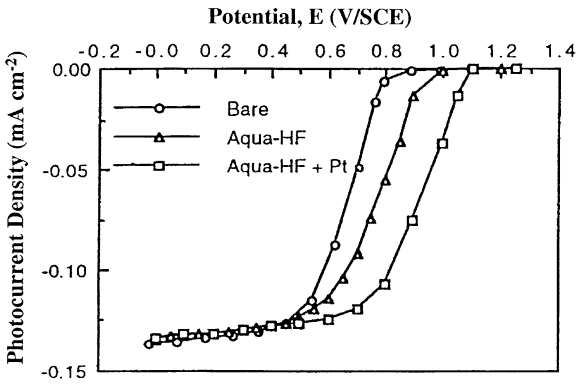

Fig. 1. The dependence of photocurrent density on potential at bare, 3 min aqua-HF treated and 5 s Pt metal islet deposited p-SiC photoelectrode. Light intensity of Xe–Hg lamp was 50 mW cm^{-2}, and the electrolyte solution was 0.50 M H_2SO_4.

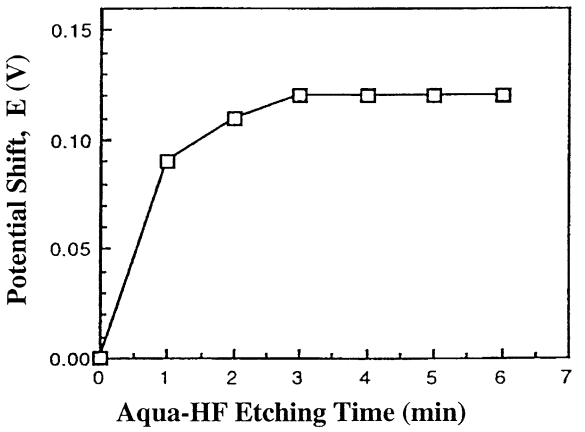

Fig. 2. The dependence of potential shift, ΔE in the j_p–E plots on the time of etching of p-SiC surface by aqua regia-HF solution. The composition of the aqua-regia-HF solution was HNO_3:HCl:HF = 1:3:4.

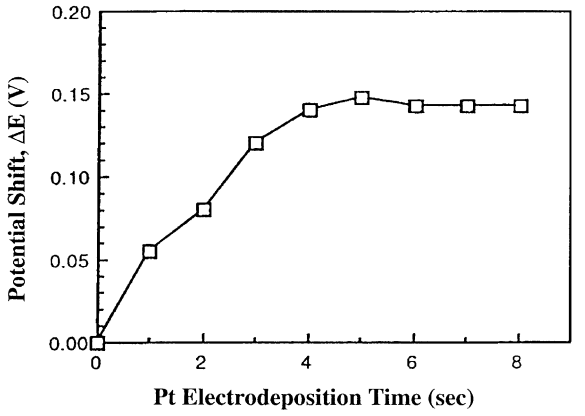

Fig. 3. The dependence of potential shift ΔE in j_p–E plots on the time of electrodeposition of Pt metal islets on p-SiC. The Pt metal was electrochemically deposited in H_2PtCl_4 (4%) solution at constant current density of 250 μA cm^{-2} under illumination of 100 mW cm^{-2}.

light. Considerable shifts of the onset potential in the j_p–E plots were observed both in the aqua-HF etched and the Pt metal islet deposited p-SiC surface (see Fig. 1). This is because at lower potential range close to onset potential the charge transfer step at the surface of p-SiC-solution interface becomes the rate determining step [14] and the charge transfer step depends on the surface condition, the catalytic nature of p-SiC surface and the surface adatoms such as Pt metal islets [9,13].

It is observed also in Fig. 1 that the limiting photocurrent density at p-SiC did not change by surface treatments. This suggests that the limiting photocurrent density is only dependent on the number of electron–hole pairs generated in the bulk and in the depletion layer of the semiconductor and at these higher potential range the transport of the photogenerated carriers inside the semiconductor becomes rate limiting [14]. Hence, the photocurrent density does not depend on the surface treatments. This observation was also reported earlier for p-Si photoelectrodes [8–10,13].

The photocurrent density observed at the single crystal p-SiC was an order of magnitude less than those observed at similar large bandgap nanocrystalline n-TiO_2 thin film electrodes [15] at the same light intensity of 50 mW cm^{-2}. This behavior may be attributed to low conductivity of single crystal p-SiC sample (2.4 Ω^{-1} cm^{-1}) and low depletion layer width (0.023 μm) and consequent high electron–hole recombination [16] and low surface area compared to nanocrystalline n-TiO_2 electrodes [15].

3.1.2. The effect of etching by aqua-regia-HF solution

Fig. 2 shows the dependence of the potential shift (ΔE) on aqua-regia-HF etching time. The highest potential shift of 0.12 V was found for etching time of 3 min, then no further potential shift was observed. However, the treatment with aqua-regia solution (HNO_3:HCl = 1:3) did not shift the onset potential in the j_p–E plots. This suggests that HF solution is necessary to remove the inactive species on the p-SiC such as SiO_2, which may have formed by oxidation in the ambient condition.

3.1.3. Effect of Pt deposition on etched p-SiC surface

Electrodeposited platinum metal islets generally act as best electrocatalyst on the surface of p-type semiconductor electrodes [9–11,17–22]. Fig. 3 shows the effect of Pt deposition time on the potential shift in the j_p–E plots. The maximum potential shift of 0.15 V was obtained at 5 s deposition time (see Fig. 3). A combined effect of aqua-HF etching and Pt deposition generated a potential shift (ΔE) of about 0.27 V compared to the untreated bare p-SiC (see Figs. 2 and 3). This shift of potential indicates the

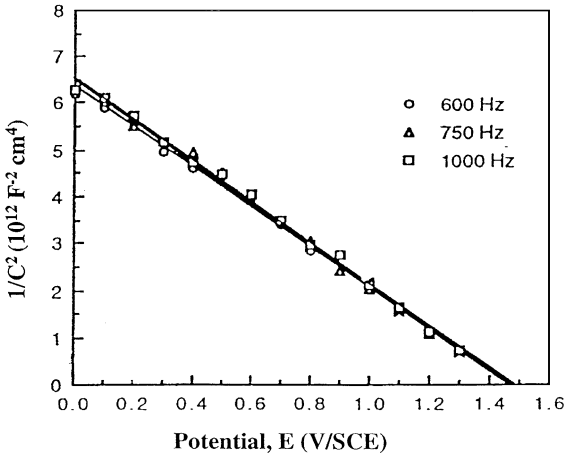

Fig. 4. Mott–Schottky plot of p-SiC measured at AC frequencies between 600 and 1000 Hz. Bare p-SiC was used for this measurement. A solution of 0.50 M H_2SO_4 and AC amplitude of 10 mV were used. All measurements were made in the dark condition. Dielectric constant of 9.7 was used for p-SiC.

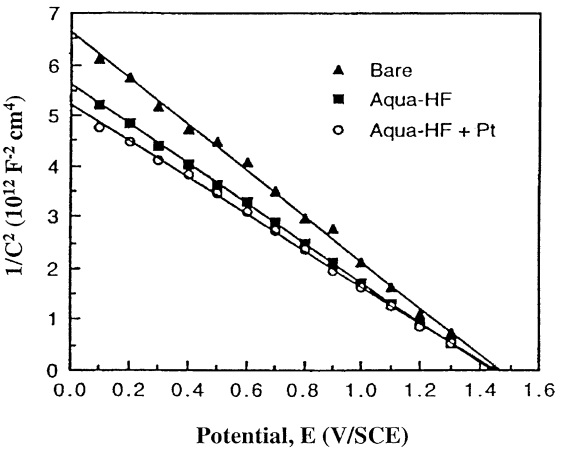

Fig. 5. Mott–Schottky plots of p-SiC measured at AC frequencies between 600 and 1000 Hz. Bare, aqua regia-HF treated and Pt metal islets deposited samples of p-SiC were used for these measurements. A solution of 0.50 M H_2SO_4 and AC amplitude of 10 mV were used. All measurements were made in the dark condition. Dielectric constant of 9.7 was used for p-SiC.

electrocatalytic effect of Pt metal islets on the p-SiC surface and as well as the effect of Schottky Junction at p-SiC and Pt metal islet interface.

3.1.4. Flat-band potential from Mott–Schottky plot

The flat band potential, E_{fb}, of a semiconductor can be obtained from the intercept of the Mott–Schottky plot using the following relation [23]:

$$(1/C^2) = (2/e_o\varepsilon_o\varepsilon N_A)(E - E_{fb} - kT/e_o), \quad (3)$$

where ε_o is the permitivity of vacuum, ε is the dielectric constant of the semiconductor, E is the electrode potential and kT/e_o is the temperature dependent term in the Mott–Schottky equation.

Fig. 4 shows the Mott–Schottky plot of bare p-SiC at frequency range between 600 and 1000 Hz in 0.5 M H_2SO_4 solution under dark condition. A constant intercept of 1.45 V SCE^{-1} was obtained at frequency between 600 and 1000 Hz, which generated the flat-band potential of 1.42 V SCE^{-1}.

3.1.5. Acceptor density of p-SiC

The acceptor density, N_A of p-SiC can be obtained from the slope of the Mott–Schottky plot as can be seen in Eq. (3). From the slope of Mott–Schottky plot (see Fig. 4) the acceptor density of about 3×10^{18} cm^{-3} is obtained (using the dielectric constant of p-SiC as 10), which agrees with the value provided by the supplier of the sample.

3.1.6. Effect of surface modification on flat-band potential of p-SiC

Fig. 5 shows the Mott–Schottky plots for the bare, aqua-HF, and aqua-HF + Pt treated p-SiC. It is observed in Fig. 5 that the intercept of the Mott–Schottky plot did not change and gave rise to flat-band potential of 1.42 V SCE^{-1} for the bare and the surface treated samples. This shows that the flat-band potential is not affected by the surface treatments of p-SiC, indicating the fact that in p-SiC the Fermi level is pinned due to its covalent character [24].

3.1.7. Quantum efficiency

The quantum efficiency under monochromatic light illumination, $Q(\lambda)$, was calculated using the following relation [25]:

$$Q(\lambda) = j_p(\lambda)/e_o I_o(\lambda), \quad (4)$$

where $j_p(\lambda)$ is monochromatic photocurrent density, e_o is the electronic charge, and $I_o(\lambda)$ is the flux of incident photon at wavelength λ.

The quantum efficiencies, $Q(\lambda)$ of p-SiC (which was treated by aqua-HF and later deposited with Pt) was determined using the $j_p(\lambda)$ values measured at an electrode potential of 0.50 V SCE^{-1} under monochromatic light illumination in Eq. (5). A very small quantum efficiency of maximum 0.9% was obtained for p-SiC at 300 nm as shown in Fig. 6. This small quantum efficiency is due to high resistance in the 1.0 mm thick p-SiC wafer (a cut from a bulk piece of p-SiC single crystal). For a hole mobility of 50 cm^2 V^{-1} s^{-1} [26], the conductivity of p-SiC can be estimated to be 2.4 Ω^{-1} cm^{-1} Furthermore, the depletion layer width can be calculated to be 0.023 μm for the acceptor density of 3×10^{18} cm^{-3} and the dielectric constant of 10 for p-SiC. This depletion layer width of 0.023 μm for p-SiC is too small compared to its absorption coefficient of light of typically 10^2 cm^{-1} at 400 nm and 3×10^4 cm^{-1} at

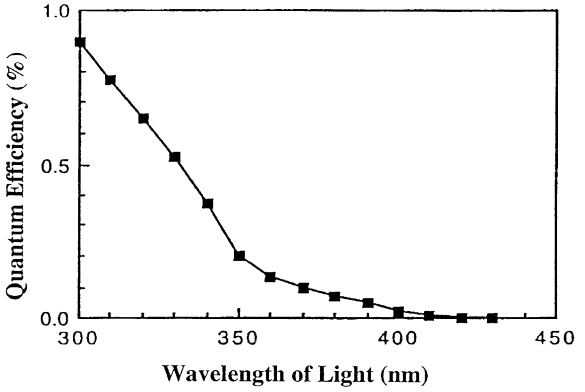

Fig. 6. The dependence of percent quantum efficiency, % $Q(\lambda)$ of p-SiC on the wavelength of light. The optimum surface treatment by aqua-HF + Pt was used. Applied potential of 0.50 V SCE^{-1} and the solution 0.50 M H_2SO_4 were used.

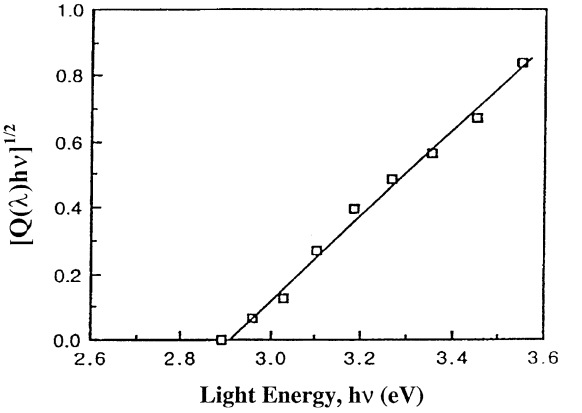

Fig. 7. Bandgap determination of p-SiC from $[Q(\lambda)hv]^{1/2}$ versus hv plot. The optimum surface treatment of aqua-HF + Pt was used. Applied potential of 0.50 V SCE^{-1} and the solution 0.50 M H_2SO_4 were used.

300 nm. Hence, most of the light photons will be absorbed in the bulk and not in the depletion layer (where field drop exists) of p-SiC semiconductor. Consequently, most of the electron–hole pairs generated by photons in the bulk were lost due to recombination before reaching the p-SiC electrode/electrolyte interface. Hence, to improve the quantum efficiency of p-SiC, it will be essential to optimize the acceptor density of p-SiC to enhance the depletion layer width.

3.1.8. Bandgap energy

The bandgap of p-SiC electrode can be determined using the following equation [25]:

$$Q(\lambda)hv = A(hv - E_g)^n, \quad (5)$$

where A is a constant, n equals either 0.5 for allowed direct transition or 2 for allowed indirect transitions. The allowed direct transition of an electron from the valence band to the conduction band by light energy, hv is not phonon assisted since such a transition does not need any change in momentum (momentum is conserved). For the indirect bandgap the transition of an electron is phonon assisted since such a transition involves change in both energy and momentum. In the case of the indirect transition, momentum is conserved via a phonon interaction, because light photons cannot provide a change in momentum [25]. Furthermore, Eq. (5) is most appropriate to use when the applied potential is far from the flatband potential, so that the transport of photogenerated carriers inside the semiconductor becomes the rate determining step [27].

The bandgap of p-SiC was determined from the intercept of the straight line obtained by plotting $[Q(\lambda)hv]^{1/2}$ versus light energy, hv using $n = 2$ in Eq. (5). A straight line was found as shown in Fig. 7, and the bandgap was found out to be 2.92 eV. This is close to the literature value of bandgap of 3.0 eV [25].

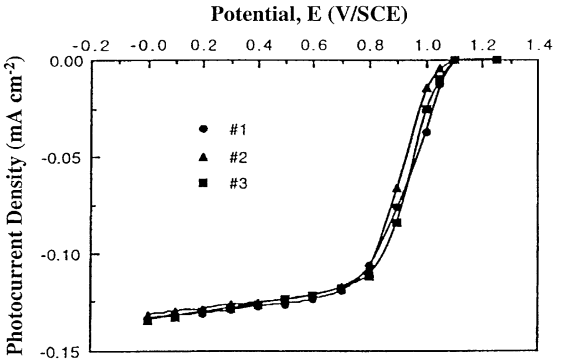

Fig. 8. Reproducibility test: the photocurrent–potential dependence at surface modified p-SiC. The surface modification of p-SiC was performed with the aqua-HF + Pt treatment. Aqua regia-HF treatment for 3 min and Pt metal islet deposition for 5 s were performed at photocurrent density of 250 μA cm^{-2}. The solution of 0.50 M H_2SO_4 and the light intensity of 50 mW cm^{-2} from the Xe–Hg lamp were used.

3.1.9. Reproducibility of results at surface modified p-SiC

The reproducibility test was performed on three aqua-regia-HF and Pt electrodeposited p-SiC samples. Fig. 8 shows j_p–E dependence of three of the p-SiC samples prepared at the same conditions. The limiting photocurrent density did not change much in three trials. However, a small variation was observed at the S curve region of the j_p–E plots. The shift in potential in this region of the j_p–E plots was ±0.02 V. At the potential of 0.00 V SCE^{-1}, the standard deviation of current density was found to be ±0.0012 mA cm^{-2}, and at 0.8 V SCE^{-1}, it was found ±0.0015 mA cm^{-2}. These small standard deviations are

within the experimental error. Also no variation of the onset potential was observed in these three trials.

3.1.10. Photoconversion efficiency

The photoconversion efficiency, ε_{eff} (photo) of light energy to chemical energy in the presence an applied potential, E_{app} under the illumination of light can be given with some modification of earlier expressions [28,29] as follows [30]:

$$\varepsilon_{\text{eff}},(\text{photo}) = [(\text{total power output}) - (\text{electrical power input})/(\text{light power input})] \times 100$$

$$= [j_{\text{p}}(E^{\text{o}}_{\text{rev}} - |E_{\text{app}}|)/(I_{\text{o}})] \times 100, \quad (6)$$

where j_{p} is photocurrent density, $E^{\text{o}}_{\text{rev}}$ is the standard reversible potential which is 1.23 V/NHE for the water-splitting reaction at pH = 0.0 and I_{o} is the intensity of incident light and $|E_{\text{app}}|$ is the absolute value of the applied potential, E_{app} which is obtained as,

$$E_{\text{app}} = (E_{\text{measured}} - E_{\text{at open circuit}}), \quad (7)$$

where E_{measured} is the electrode potential at which the photocurrent density, j_{p} was measured and $E_{\text{at open circuit}}$ is electrode potential at open circuit condition under the same illumination of light used for the determination of photocurrent density, j_{p}.

One should note that the input power from the applied potential does not produce photocurrent. The photocurrent is observed only when the electrode is illuminated by light. This means that the input power for photocurrent is the intensity of light, I_{o} only. Because the photocurrent is equal to illumination current −dark current, one should not include any contribution of input power using $j_{\text{p}}E_{\text{app}}$ term in the denominator of Eq. (6).

However, non- self-driven photoelectrochemical cells (PEC) cannot generate enough photopotential equal to or greater than the reversible potential for the reaction, $E^{\text{o}}_{\text{rev}}$. Consequently, an applied potential, E_{app} is needed to help out such PEC to overcome some portion of the thermodynamic barrier, $E^{\text{o}}_{\text{rev}}$ and the overpotentials for the reaction. This means that the cell does not work at $E^{\text{o}}_{\text{rev}}$ but work at $(E^{\text{o}}_{\text{rev}} - E_{\text{app}})$. Hence, the power output of the non-self-driven PEC will be $j_{\text{p}}(E^{\text{o}}_{\text{rev}} - E_{\text{app}})$ and the power input for the photocurrent generation is the intensity of light, I_{o} only as it was expressed in above Eq. (6).

A plot of the photoconversion efficiency, ε_{eff}, (photo) for the aqua-HF treated and Pt metal islet deposited p-SiC versus applied potential, E_{app} using Eqs. (6) and (7) is shown in Fig. 9. Since p-SiC requires small external potential to initiate the reaction, the photoconversion efficiency starts increasing at close to 0.0 V SCE^{-1}. However, due to large bandgap energy of p-SiC, the conversion efficiency was found small. Using $E^{\text{o}}_{\text{rev}} = 1.23$ V in Eq. (6) for the water-splitting reaction, the highest photoconversion efficiency of 0.17% at the applied potential, $E_{\text{app}} = 0.45$ V was observed (see Fig. 9). The intensity of

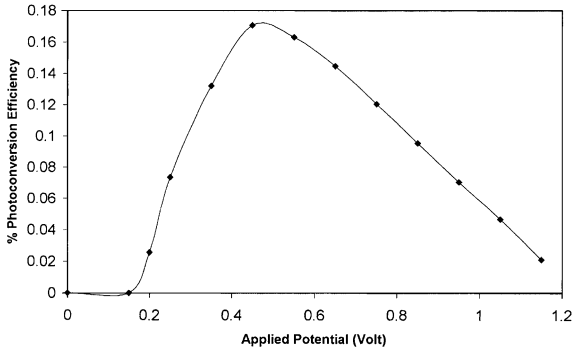

Fig. 9. A plot of photoconversion efficiency of light energy to chemical energy versus electrode potential [at p-SiC in 0.5 M H_2SO_4 solution using $E_{\text{rev}} = 1.23$ V and the open circuit potential, $E_{\text{open circuit}} = 1.25$ V SCE^{-1}. The surface modifications were performed with aqua regia-HF solution for 3 min and Pt metal islet deposition for 5 s at 250 μA cm^{-2} using light intensity of 50 mW cm^{-2}.

light $I_{\text{o}} = 50$ mW cm^{-2} were used. However, the photoconversion efficiency of nanocrystalline n-TiO_2 were found 2.0% [15] compared to 0.17% at p-SiC due to high recombination of photo-generated carriers in the latter due to its covalent character.

3.1.11. Total conversion efficiency

The total conversion efficiency of light and electrical energy to chemical energy, ε_{eff}(total) in the presence of an external applied potential or built-in potential under the illumination of light can be given as follows [28–30]:

$$\varepsilon_{\text{eff}}(\text{total}) = [(\text{total power output})/(\text{light power input})] \times 100$$

$$= [(j_{\text{p}}E^{\text{o}}_{\text{rev}}/(I_{\text{o}})] \times 100. \quad (8)$$

From Eq. (8) total conversion efficiency of 0.27% was obtained for the observed photocurrent density of 0.11 mA cm^{-2} at the surface treated p-SiC at the electrode potential, $E = 0.8$ V SCE^{-1} under the illumination of light of intensity $I_{\text{o}} = 50$ mW cm^{-2}.

The photoconversion efficiency of a self driven or built-in potential driven PEC involving two photoelectrodes can be expressed as

$$\varepsilon_{\text{eff}}(\text{photo}) = [(j_{\text{p}}E^{\text{o}}_{\text{rev}}/(2I_{\text{o}})] \times 100. \quad (9)$$

Note that 2 appears in the denominator of Eq. (9) when two photoelectrodes of equal sizes are put side by side facing the light source. However, it is important to note that the factor 2 will not be needed in the denominator of Eq. (9) if two photoelectrodes of equal sizes were put at an angle of 60° facing the light source.

3.2. The p-SiC/n-TiO_2 photoelectrochemical cell

The combination of single crystal p-SiC and nanocrystalline n-TiO_2 (reported earlier [15]) photoelectrodes was tested to determine whether this can act as a self-driven system for water-splitting reaction under illumination of light. The p-SiC was etched with aqua-regia-HF for 3 min and platinized for 5 s. The area of each electrode was 0.25 cm^2. Both photoelectrodes (p-SiC and n-TiO_2) were placed side by side facing the light source. The electrolyte was 0.5 M H_2SO_4. The open circuit potential under illumination of light was found to be 1.24 V between n-TiO_2 and p-SiC photoelectrodes. This potential of 1.24 V is just sufficient to split water. Under illumination, the close circuit potential between n-TiO_2 and p-SiC was found to be 0.23 V. The photocurrent density observed at this closed circuit potential was found to be 0.05 mA cm^{-2} indicating the fact that the p-SiC/n-TiO_2 combination can photosplit water without the use of any external applied potential.

The combination of p-SiC and n-TiO_2 exemplify the situation where a large overlap of band positions between p- and n-type semiconductors occurs. However, at the short circuit condition the small photocurrent density of 0.05 mA cm^{-2} was observed in spite of large overlap of band positions between these two semiconductors and also with the hydrogen and oxygen evolution potentials [7]. Using Eq. (10), the cell photocurrent density of 0.05 mA cm^{-2} and the light intensity of 50 mW cm^{-2} the photoconversion efficiency was found to be 0.06% for the self-driven p-SiC/n-TiO_2 system. This small photocurrent density and the photoconversion efficiency of this self-driven system can be attributed to large bandgap energy of these semiconductors and as well as high recombination rate of the photogenerated carriers in the covalent bonded p-SiC.

In summary it is important to point out that

1. It was possible to shift the onset potentials of p-SiC by surface treatments with the aqua-HF and also by electrodeposited Pt metal islets.
2. The elecrode potential of p-SiC at opencircuit condition did not change with different surface treatments or by Pt metal islet deposition.
3. The rate determining step at electrode potentials close to onset potential is the charge transfer at the p-SiC electrode-solution interface, and this charge transfer rate improved by surface treatments. As the surface becomes more active by the surface treatment, the external potential required to initiate the hydrogen evolution reaction decreased, consequently, shifted the onset potential to more positive potential in the j_p–E plots.
4. The combination of p-SiC and the n-TiO_2 can act as a self-driven system to photosplit water without the use of any external bias potential due to their suitable band positions for the hydrogen and oxygen evolution reactions, but the efficiency was low due to their high bandgap energy and as well as high recombination rate in the covalent bonded p-SiC.
5. As this combination, p-SiC/n-TiO_2 was found, in this study, to split water as a self-driven cell, future studies should be focused in improving the efficiency by utilizing proper sensitizer on these high bandgap semiconductor surfaces.

Acknowledgements

We gratefully acknowledge the partial financial support of this work by the ALCOA Foundation, and we also acknowledge the donation of single crystal samples by Sandia National Laboratory, New Mexico.

References

[1] Gloria M, Memming R. J Electroanal Chem 1975;65:163.
[2] Crok RL, McDuff RC, Sammell AF. J Electroanal Chem 1998;135:3069.
[3] Yamamura S, Kojima H, Joda J, Kawai W. J Electrochem Soc 1987;225:287;
Yamamura S, Kojima H, Joda J, Kawai W. J Electrochem Soc 1988;247:333.
[4] Inoue T, Yamase T. Chem Lett 1985;7:869.
[5] Memming R. Photochem Photobiol 1972;16:325.
[6] Lauermann I, Memming R, Meissner D. J Electrochem Soc 1997;144:73.
[7] Memming R. In: Conway BE, Bockris JO'M, Yeager E, Khan SUM, White RE, editors. Comprehensive treatise of electrochemistry, vol. 7. New York: Plenum Press, 1983. p. 529.
[8] Szklarczyk M, Bockris JO'M, Brusic V, Sparow G. Int J Hydrogen Energy 1984;9:707.
[9] Szklarczyk M, Bockris JO'M. J Phys Chem 1984;88:1808.
[10] Szklarczyk M, Bockris JO'M. Chem Phys Lett 1983;42:103.
[11] Contractor AQ, Bockris JO'M. Electrochem Acta 1987;32:121.
[12] Szklarczyk M, Bockris JO'M. J Phys Chem 1984;88:5241.
[13] Khan SUM, Majumder SA. Int J Hydrogen Energy 1989;14:653.
[14] Khan SUM, Bockris JO'M. J Phys Chem 1984;88:2504.
[15] Khan SUM, Akikusa J. J Electrochem Soc 1998;145:89.
[16] Kalinina V, Kholuyanov GF, Shchukarcv AV, Savkina NS, Bbanin AI, Yagovkina MA, Kuznetsov NI. Diamond Related Mater 1999;8:1114.
[17] Choi YK, Seo SS, Chio KH, Choi QW, Park SM. J Electrochem Soc 1992;139:1803.
[18] Kainthla RC, Zelenay B, Bockris JO'M. J Electrochem Soc 1986;133:248.
[19] Kainthla RC, Zelenay B, Bockris JO'M. J Electrochem Soc 1987;134:841.
[20] Bockris JO'M, Szklarczyk M, Contractor AQ, Khan SUM. Int J Hydrogen Energy 1984;9:741.
[21] Kainthla RC, Khan SUM, Bockris JO'M. Int J Hydrogen Energy 1987;12:381.

[22] Verpoort PJ, Vermeir IE, Gomes WP. J Electrochem Soc 1996;142:3589.
[23] Gleria M, Memming R. J Electroanal Chem 1975;65:163.
[24] Rysy S, Sadownski H, Helbig R. J Solid State Electrochem 1999;3:437.
[25] Pankove JI. Optical processes in semiconductor. New York: Dover Pub., 1971 [Chapter 3].
[26] Sze SM. Physics of semiconductor devices. New York: Wiley, 1981. p. 849.
[27] Bockris JO'M, Khan SUM. Surface electrochemistry. New York: Plenum Pub. Corp., 1993 [Chapter 5].
[28] Khan SUM, Majumder SA. Int J Hydrogen Energy 1994;29:881.
[29] Bockris JO'M, Murphy OJ. App Phys Comm 1983;2:203.
[30] Khan SUM, Akikusa J. J Phys Chem B 1999;103:2184.